Barrier Coverage of Line-Based Deployed Wireless Sensor Networks

Anwar Saipulla † Cedric Westphal * Benyuan Liu † Jie Wang †

† Department of Computer Science
University of Massachusetts Lowell
Lowell, MA 01854, USA
{asaipull, bliu, wang}@cs.uml.edu

* DoCoMo Labs USA
3240 Hillview Avenue
Palo Alto, CA 94304, USA
cwestphal@docomolabs-usa.com

***Abstract*— Barrier coverage of wireless sensor networks has been studied intensively in recent years under the assumption that sensors are deployed uniformly at random in a large area (Poisson point process model). However, when sensors are deployed along a line (e.g., sensors are dropped from an aircraft along a given path), they would be distributed along the line with random offsets due to wind and other environmental factors. It is important to study the barrier coverage of such line-based deployment strategy as it represents a more realistic sensor placement model than the Poisson point process model. This paper presents the first set of results in this direction. In particular, we establish a tight lower-bound for the existence of barrier coverage under line-based deployments. Our results show that the barrier coverage of the line-based deployments significantly outperforms that of the Poisson model when the random offsets are relatively small compared to the sensor's sensing range. We then study sensor deployments along multiple lines and show how barrier coverage is affected by the distance between adjacent lines and the random offsets of sensors. These results demonstrate that sensor deployment strategies have direct impact on the barrier coverage of wireless sensor networks. Different deployment strategies may result in significantly different barrier coverage. Therefore, in the planning and deployment of wireless sensor networks, the coverage goal and possible sensor deployment strategies must be carefully and jointly considered. The results obtained in this paper will provide important guidelines to the deployment and performance of wireless sensor networks for barrier coverage.**

Keywords: coverage, wireless sensor networks, deployment strategies.

I. Introduction

Coverage problems, including point coverage, area coverage, and barrier coverage, are important problems in wireless sensor networks. Differing from point coverage that covers specific points of interest and from area coverage that covers the entire region, barrier coverage aims at detecting intruders that attempt to cross the network. It requires a chain of sensors across the deployed region with the sensing areas of adjacent sensors overlapping with each other [1]. Each independent chain of sensors is referred to as a barrier, acting as a "trip wire" to detect intruders attempting to cross the network.

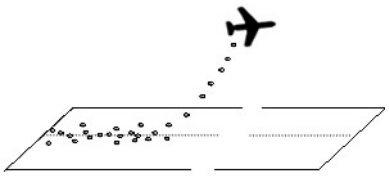

Fig. 1. A line-base deployed wireless sensor network. Actual landing points of sensors may deviate from their targeted locations because of environment factors.

Sensor deployment strategies have direct impact on barrier coverage. Placing sensors side by side regularly along straight lines across the region is the best one would hope to achieve [2], for it is simple and offers the most efficient possible barrier coverage. But it is infeasible to achieve in most applications. When deploying sensors to monitor boundaries of battlefields, country borders with complex terrains, or other hard-to-reach areas, we may have to rely on other deployment methods. These methods may include dropping a large number of sensors from vehicles such as aircrafts along predetermined routes [3], [4], as illustrated in Figure 1. When dispersed from an aircraft, sensors will most likely land at locations deviating from their targeted landing points with random offsets because of mechanical inaccuracy, wind, terrain characteristics, and other environmental factors.

Most of the early research on barrier coverage assumes that the sensor locations follow a Poisson point process, where sensors are uniformly distributed in a vast region [2], [5], [6]. While it may be appropriate for certain deployment strategies, this model of uniform distribution does not capture the sensor distributions under the airdrop deployment strategy. Consequently, analytical results derived from such models are not applicable to line-based sensor deployments. Sensors deployed from aircrafts tend to be concentrated along the deployment line with some random offsets. We assume that the random offset of each sensor from its target landing point follows a normal distribution. For convenience, we refer to this type of distribution as *line-based normal random offset distribution* (LNRO) hereafter.

The existence and number of sensor barriers depends on a number of factors, including the number of sensors, sensing range of each sensor, and the variance of the normally distributed random offsets. Using mathematical analysis we first establish a tight lower bound for the existence of barrier coverage under LNRO. We then compare the quality of barrier coverage of sensor deployment under LNRO with that under Poisson point process. Our results show that the barrier coverage under the two deployment strategies are significantly different from each other, with LNRO outperforming Poisson point process when the variance of the random offset in LNRO is relatively small compared to the sensor's sensing range. This is because, in LNRO, sensors are concentrated along the deployment lines rather than uniformly distributed as in a Poisson point process, providing a better chance for barriers to be formed. Finally, we study the multiple-line deployment scenario and investigate how barrier coverage depends on the distance between adjacent lines and the random offsets of sensors.

Our results demonstrate that sensor deployment strategies have direct impact on the barrier coverage of wireless sensor networks. Different deployment strategies can result in significantly different barrier coverage. Therefore, in the planning and deployment of wireless sensor networks, the coverage goal and possible sensor deployment strategies must be carefully examined. The results obtained in this paper will provide important guidelines to the deployment and performance of wireless sensor networks for barrier coverage.

The rest of the paper is organized as follows. Section II reviews previous work on barrier coverage of sensor networks. In Section III we describe the network model and define barrier coverage. In Section IV we derive the probability of the existence of a barrier under LNRO. We also provide a comparison between the theoretical lower-bound results and the actual simulation results. In Section V we compare the barrier coverage quality achieved by sensors deployed under LNRO with that under Poisson point processes. In Section VI we present a multiple-line deployment strategy, and simulate large-scale multiple-line deployment scenarios to show its properties. We conclude the paper in Section VII.

II. Related Work

The notion of barrier coverage, first introduced in the context of robotic sensors [1], concerns a sensor network's capability to detect intruders crossing from one side of the network region to the opposite side. There are a number of different barrier coverage measures that have been studied.

Path coverage is defined in [7] and efficient algorithms are proposed to find the maximum breach path between two end points that are least or most likely to be detected by sensors. The notion of path exposure is introduced in [7] to measure the likelihood that an intruder is detected when moving along a given path. A centralized algorithm is proposed to find minimum exposure paths, where the probability of an intruder being detected is minimized. These path coverage problems are further studied in [8], [9] and efficient distributed algorithms are devised. In [10], T. Clouqueur et al. investigated the detection of intruders traversing the region using collaborative detection schemes among sensors. In [11], E. Amaldi et al. proposed an optimization framework for selecting sensor positions to detect mobile targets traversing a given area.

Liu and Towsley [12] first studied the barrier coverage of two-dimensional plane and two-dimensional strip sensor networks using percolation theory. The barrier coverage of a two-dimensional plane network is related to the existence of a giant sensor cluster that percolates the network. For a two dimensional strip network of finite width, they prove that there always exists a crossing path along which an intruder can cross the strip undetected. They also characterize the probability that an intruder can be detected when crossing a strip.

Kumar, Lai, and Arora [2] introduced the notion of weak coverage, devised a centralized algorithm to determine whether a region is weakly k-barrier covered, and derived the critical conditions for weak barrier coverage in a randomly deployed sensor network. Chen, Kumar, and Lai [5] later devised a localized algorithm that guarantees the detection of intruders whose trajectory is confined to a slice of the belt region of deployment. In

[13], Balister, Bollobas, Sarkar, and Kumar introduced new techniques for deriving reliable density estimates to achieve barrier coverage in finite regions. Recently, Liu, Dousse, Wang, and Saipulla [6] derived the critical conditions for strong barrier coverage and devised efficient algorithms to construct strong sensor barriers. In [14], Chen, Lai, and Xuan studied how to measure and guarantee the quality of barrier coverage in wireless sensor networks.

III. Network Model

We assume that sensors are deployed in a two-dimensional rectangular area of length l and width h (see Figure 2), where sensors do not move after they are deployed. We assume that each node knows the coordinates (x,y) of its own location. This may be done using an on-board GPS unit or other localization mechanisms.

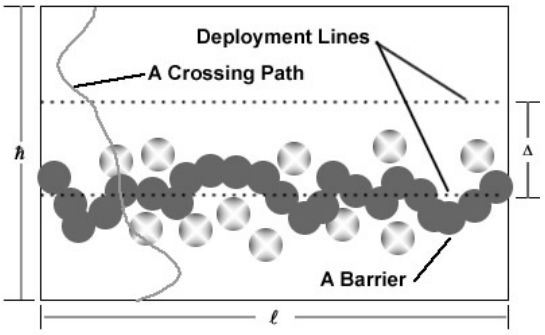

Fig. 2. Sensors are deployed in a rectangular area of $l \times h$. The distance between adjacent deployment lines is Δ.

Let $f(x,y)$ denote the probability density function (pdf) of the sensor location. Then

$$f(x,y) = \begin{cases} \frac{1}{lh}, & 0 \le x \le l,\ 0 \le y \le h, \\ 0, & \text{otherwise.} \end{cases}$$

For the line-based deployment strategy, we assume that there are $m \ge 1$ horizontal deployment lines along the length of the rectangle. When $m > 1$, we assume that these lines are evenly spaced, with a distance Δ between each pair of adjacent lines. Let y_j denote the vertical coordinates of the j-th deployment line, where $0 \le j < m$. We have

$$y_j = y_0 + j\Delta.$$

We assume that along each line, sensors are to be evenly distributed. Let n be the number of sensors to be distributed along a given line. Let $\zeta = l/(n+1)$. The horizontal coordinates of the i-th target landing point is

$$x_i = \frac{il}{n+1} = i\zeta,\ 1 \le i \le n.$$

Because of mechanical inaccuracy, wind, terrain constraints, and other environmental factors, the actual landing point of each sensor will deviate from its target by a random offset. Denote by δ_i^x and δ_i^y the offset of sensor s_i in the horizontal and vertical directions, respectively. On the j-th dropping line, the actual landing point of sensor s_i is thus $(x_i + \delta_i^x, y_j + \delta_i^y)$.

In practice, the random offsets of nearby sensors are usually correlated. To simplify the analysis and provide insight, we assume that the random offsets are independently and identically distributed (i.i.d.) with a normal distribution of zero mean and variance σ^2, i.e.,

$$\delta_i^x, \delta_i^y \sim N(0, \sigma^2).$$

Note that our later analysis can be easily generalized to the case where δ_i^x and δ_i^y does not share the same standard deviation σ.

We adopt the widely-used binary disk sensing model. Each sensor has a sensing range r and can detect any intruders within its sensing range. Let s be a sensor that has been deployed. For convenience, we also use s to denote the sensor's location, which is the center of its sensing range. Two nodes are said to be connected if their sensing areas overlap. In other words, node s_i is connected to node s_j if and only if $|s_i - s_j| \le 2r$, where $|s_i - s_j|$ represents the Euclidean distance between the two sensors. A sensor barrier is formed by a set of connected sensors that intersect both of the left and right boundaries of the rectangular. Obviously no intruders can cross such a sensor barrier without being detected.

A *crossing path* is a path that connects one side of the region to the opposite side, where the ingress point and the egress point reside on two opposite sides of the region. We assume that the intruders attempt to cross the region along the width of the rectangular area.

We measure the strength of the barrier coverage in a sensor network by the number of disjoint barriers in the network. A path is said to be k-covered if it is intercepted by at least k distinct sensors. We say that an event on n sample points occurs with high probability (w.h.p.) if its probability tends to 1 as $n \to \infty$. We now formally define strong barrier coverage.

Definition 1: A sensor network is strongly k-barrier covered if

$$P(\text{any crossing path is } k\text{-covered}) = 1 \text{ w.h.p.} \qquad (1)$$

Kumar, Lai, and Arora [2] introduced the notion of weak barrier coverage, which guarantees detections of intruders moving along congruent crossing paths. But it does not guarantee detection of intruders moving along arbitrary crossing paths as guaranteed by strong barrier coverage. We will focus on strong barrier coverage in this paper. For convenience, we will use barrier coverage to refer to strong barrier coverage.

IV. Probability Analysis of Barrier Coverage

In this section we first present the assumptions and the corresponding analytical results for the probability of barrier coverage under LNRO. We then validate our analysis via simulations.

A. Assumptions and Results

We first consider the probability that a single line deployment constitutes a barrier. That is, we consider a single line of n nodes s_i with coordinates $(x_i+\delta_i^x, \delta_i^y)$, $1 \le i \le n$, where $x_i = i\zeta$ and δ_i^x and δ_i^y are random variables in a normal distribution with the same standard deviation σ. Our analysis can be adapted to the case where $\sigma^x \neq \sigma^y$ in a straightforward manner. Recall that two nodes are connected if their distance is less than $\rho \triangleq 2r$. Also notice that, without loss of generality, we assume that $y_i = 0$ for all the nodes for convenience.

We make the following assumptions:

1) Nodes are deployed so that the distance between adjacent targeted positions is within the sensing range of the two sensors. This means that $\rho > \kappa\zeta$, for some factor $\kappa > 1$ that we will specify later. Intuitively, we want to avoid the case where ρ is too close to $l/(n+1)$, for otherwise only small perturbation could create breaches in the barrier. We expect this assumption to be reasonable for many application scenarios as typical barrier coverage applications use sensors with large sensing ranges. For example, for MSP410CA wireless security system by XBow [15], the magnetic field sensors and infrared sensors have a sensing range of about 60 feet and 80 feet, respectively.
2) $\sigma << \zeta$. This assumption means that we still exert some control over the position of the nodes. The perturbation of the node position stays relatively small with respect to the gap between two nodes. We will see in the evaluation that our analysis stays valid with a standard deviation σ equal to 20% of the targeted gap between two sensors ζ.

We can now state our result:

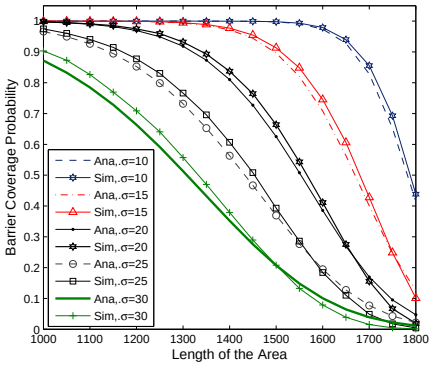

Fig. 3. Probability of Barrier Coverage for various area lengths with 9 nodes and $\rho = 200$. From left to right, $\sigma = 30, 25, 20, 15, 10$.

Theorem 4.1: **When assumption 1) and 2) are satisfied, the probability that barrier coverage exists for a single line by covered by n sensors with coordinates $(i\zeta + N(0,\sigma^2), N(0,\sigma^2)), 1 \le i \le n$, and sensing range $r = \rho/2$ is given by**

$$P(\text{BarrierCoverage}) \gtrsim \left[1 - Q_1\left(\frac{\zeta}{\sqrt{2}\sigma}, \frac{\rho}{\sqrt{2}\sigma}\right)\right]^{(n+1)}, \quad (2)$$

where

$$Q_1(s,t) = e^{-\frac{s^2+t^2}{2}} \sum_{k=0}^{\infty} \left(\frac{s}{t}\right)^k I_k(st) \quad (3)$$

and I_k is the k-th order modified Bessel function of the first kind.

The proof of the theorem is presented in the appendix. In the next section we will show that, through a large number of numerical experiments, the lower bound given in inequality (2) is tight.

B. Probability of Barrier Coverage: Analysis vs. Simulation

Figure 3 plots the probability of barrier coverage for a single line deployment with a two-dimensional Gaussian perturbation with standard deviation σ. In the simulation, the length l is varied from 1,000 to 1,800 meters for a single line deployment. Nine nodes of sensing range $r = 100$ meters are deployed along the line. Thus the connectivity radius is $\rho = 200$ meters, and the distance between adjacent target positions, ζ, varies between 100 and 180 meters, satisfying Assumption 1). We vary the standard deviation σ between 10 and 30, which meets the requirement of Assumption 2). The curves from left to right correspond to the reversed order of the chosen standard deviations, i.e., $\sigma = 30.$ 25, 20, 15, and 10.

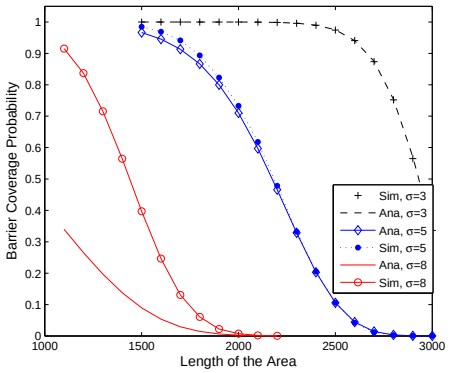

Fig. 4. Probability of Barrier Coverage for various area lengths with 99 nodes and $\rho = 40$. From left to right, $\sigma = 8, 5, 3$.

It can be observed that there is a good match between the simulation results and our analysis. The match improves as the variance decreases. One can also verify that the analysis is indeed a lower bound as long as Assumption 1) is satisfied, i.e., as long as ρ stays larger than $\kappa\zeta$, where κ is in the range of 1.05 for $\sigma = 10$ to 1.33 for $\sigma = 30$.

The good match between the analysis and the simulation is insensitive to the number of nodes, as can be observed from Figure 4, where the number of nodes has been increased to 99, and ρ reduced to 40 meters. The corresponding ζ varies between 11 and 30. Recall that Assumption 2) requires that the standard deviation be a relatively small fraction of ζ. For the leftmost pair of curves in Figure 4, ζ varies between 11 and 22, and the standard deviation is $\sigma = 8$. This breaks Assumption 2), and indeed, the match is poor between the analysis and the simulation. However, when we decrease σ to 5 and 3, simulation and analysis starts to track each other very well again.

V. Comparison with Poisson Model

Most previous studies on barrier coverage consider the nodes distributed according to a Poisson process or a uniform distribution in the area to be covered. We now compare our results with the barrier coverage probability for a Poisson process.

A. Comparison with Two-dimensional Poisson Model

In the case of uniform distribution, each sensor has the equal likelihood to be located at any point in the rectangle. Thus, the sensors are spread out rather evenly in the area. It has been proved in [6] that in the asymptotic case, barriers exist if and only if the width of the rectangle is larger than the logarithm of the length and at the same time the sensor density λ is greater than some critical value. In the line-based deployment

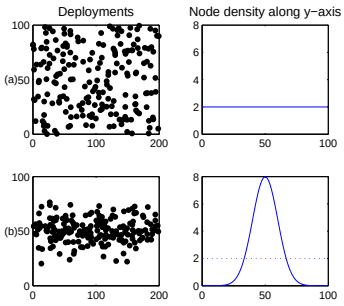

Fig. 5. 200 Sensors deployed based on uniform distribution and line-based normal distribution, and the corresponding sensor density on y-axis. (a)Uniform distribution, λ = 0.02; (b)Single-line LNRO, σ = 10.

strategy with normally distributed random offsets, sensors are concentrated along the deployment line. The node density in the vertical direction forms a "bell" curve whose shape is determined by the variance of the normal distribution. Figure 5 illustrates the deployment layouts of the uniform distribution and line-based normal distribution, and the corresponding sensor densities in the vertical direction.

Compared to the uniform distribution, sensors are concentrated along deployment lines in the line-based deployment strategy, providing a better chance for barriers to be formed. To compare the barrier coverage of LNRO with that of the Poisson point process, we note that 99.7% of the sensors fall within the distance of 3σ from the deployment line in LNRO, and so we choose the width of the rectangle for the uniform distribution to be 6σ for comparison.

For the Poisson point process deployment, the probability that the nodes provides barrier coverage is given by [13]. We repeat here the key result of [13]. Define a strip of width h and length l. Nodes are distributed according to a Poisson process with density λ and have a connectivity radius ρ. To make the comparison between the LNRO distribution and the Poisson point process fair, we set h to be equal to a multiple of σ.

Define the break density to be $I_{h,\rho,\lambda}$. With the proper definition, breaks in the coverage can be shown to follow a Poisson distribution as well, and thus the density of this Poisson process is $I_{h,\rho,\lambda}$. The probability that the strip provides barrier coverage is thus equal to the probability that there is no break, which is equal to:

$$P(\text{Barrier Coverage}) = e^{-lI_{h,\rho,\lambda}} \tag{4}$$

$I_{h,\rho,\lambda}$ can be approximated by:

$$\begin{aligned} I_{h,\rho,\lambda} &= \sqrt{\lambda} I_{h\sqrt{\lambda},\rho\sqrt{\lambda}} \text{ where} \\ I_{a,b} &= e^{-\alpha_a b - \beta_b} \text{ and} \\ \alpha_a &= a - 1.12794 a^{-\frac{1}{3}} - 0.20 a^{-\frac{5}{3}} \\ \beta_b &= -\frac{1}{3}\log(b) + 1.05116 + 0.27 b^{-\frac{4}{3}} \end{aligned} \quad (5)$$

One requirement to study the barrier coverage with a Poisson process is to assume that $\lambda > \lambda_c$, where λ_c is the critical density for percolation. In other words, λ should be in the supercritical regime. For a network of size $l \times h$, we have $\lambda = \frac{n}{hl}$. If we set $h = 6\sigma$, with $\sigma = 10$, then $\lambda = 0.00015$. The critical density, when $\rho = 200$, is $\lambda_c = 0.0772$. (The critical density depends on the connectivity radius in such manners that the average number of neighbors is equal to 4.5118 for the Gilbert model [16]). One would need to narrow down the strip to a width $h = \sigma/86$ to achieve super-criticality of the Poisson process. And indeed, either using Equation (5) or simulating the deployment according to a Poisson process with $\lambda = 0.00015$, $h = 6\sigma$, $\sigma = 10$, $n = 9$ and $l = 1000$ shows that barrier coverage is achieved with a negligible probability.

Even in the supercritical regime, the probability of barrier coverage is very small for the Poisson process compared to that of the LNRO deployment. Figure 6 compares the LNRO and Poisson process in an area of length varying between 1500 and 5000m. The LNRO deployment, with 99 nodes, $\rho = 100$ and a standard deviation of $\sigma = 10$ ensures barrier coverage with probability close to one, both in the analytical model and the simulated model, across the whole range of l. The Poisson process, in a strip of size $l \times \sigma$ (note that the LNRO deployment is 97% contained within a strip of size $l \times 6\sigma$, thus in a much wider strip), has on average 99 nodes with $\rho = 100$. The parameters are chosen so that λ is firmly supercritical (in the Gilbert model) for all values of l. Figure 6 shows both simulation and analysis from equation (5) for the Poisson deployment, with a much lower probability of barrier coverage, despite the favorable parameters.

B. Comparison with One-dimensional Poisson Model

In LNRO, sensors are concentrated along the deployment line with random offsets. Thus, it is also interesting to compare the barrier coverage of LNRO with that of a strict line deployment where all sensors fall on the same line ($\sigma^y = 0$).

Figure 7 compares the probability of barrier coverage of LNRO with that of a line distribution according to

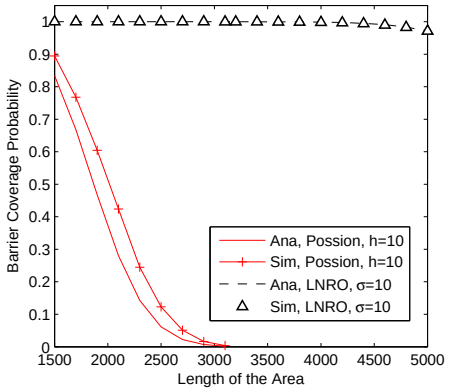

Fig. 6. Probability of Barrier Coverage for various area lengths with 99 nodes, $\rho = 100$, $h = 10$ for the Poisson deployment and $\sigma = 10$ for the LNRO deployment.

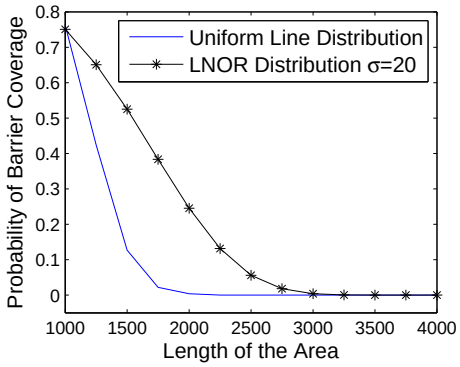

Fig. 7. Probability of Barrier Coverage for various area lengths with 50 nodes, $\rho = 100$, for a uniform sensor distribution on a line, and for a two-dimensional LNRO deployment with $\sigma = 20$.

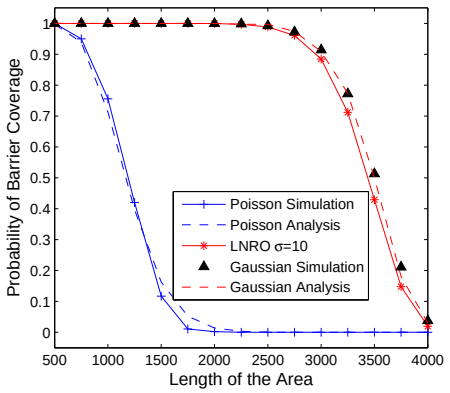

Fig. 8. Probability of Barrier Coverage for various area lengths with 50 nodes, $\rho = 100$, for a distribution of sensors on a line along a Poisson distribution, for a regular distribution with a Normal(0,10) perturbation (Gaussian) along the x-axis, and for a two-dimensional LNRO deployment with $\sigma = 10$.

a uniform line distribution. For a given line segment of length l, the corresponding probability density function (pdf) of a node location in the strict line deployment is $P(x) = 1/l$, when $x \in [0,l]$, and 0 otherwise. In the simulation, we set $\rho = 100$, $\sigma = 20$, $n = 50$, and l from 1000 to 5000. It can be observed that the barrier coverage of LNRO consistently outperforms that of single line uniform case. Reducing the variance in the y-dimension (σ_y) in LNRO will further increase the barrier coverage probability of LNRO, resulting in better performance over the single line uniform distribution. Simulations show a relatively similar probability of barrier coverage for a Poisson point process and for a uniform distribution with the same average number of nodes.

For the uniform distribution along a single line, a similar analysis to that of Theorem 4.1 shows that, under the Assumptions 1) & 2), the barrier coverage probability for the Poisson case is given by

$$P(\text{Barrier Coverage}) = \left(1 - e^{-\frac{n\rho}{l}}\right)^n. \quad (6)$$

We also consider a strict line deployment with Normal perturbation along the line. In this case we have $\sigma_y = 0$, and $x_i = i\zeta + N(0,\sigma_x)$. Similar analysis as for Theorem 4.1 shows that

$$\begin{aligned} P(\text{Barrier Coverage}) &= \left(P(N(n/l, \sqrt{2}\sigma) < \rho)\right)^n \\ &= \left(\frac{1}{2} + \frac{1}{2}\text{erf}(\frac{\rho - \zeta}{2\sigma})\right)^n \quad (7) \end{aligned}$$

Figure 8 plots numerical results of Equations 6 and 7 with the corresponding simulation results. For reference, the LNRO case is also included. It can be observed that for both cases the analysis matches the simulation results very well. Also, the barrier coverage of LNRO and the line deployment with Normal perturbation are close to each other, both outperforming the line deployment with Poisson distribution.

VI. Barrier Coverage of Multiple-Line Deployments

Deploying sensors along multiple lines may provide robustness and multiple lines of defense in the deployed region. In this part, we consider a two-line deployment scenario to focus on the effects of two deployment parameters: the standard deviation (σ) of the deployment random offset and the distance between the two deployment lines (Δ). Figure 9 depicts two-line deployment scenarios with different Δ values.

We use a modified Maximum Network Flow algorithm to calculate the number of disjoint barriers in a network.

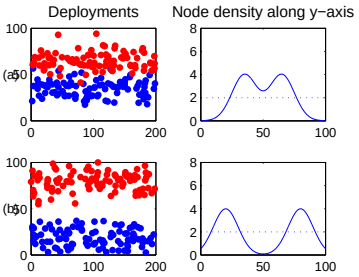

Fig. 9. Sensor distributions of two-line deployment scenarios, and the corresponding sensor densities in the vertical direction. σ = 10 meters. (a) Δ = 30 meters ; (b) Δ = 60 meters.

This algorithm can also be used to find disjoint barriers. Details of the algorithm is provided in the appendix.

In the following experiments, a total number of 10,000 sensors are deployed along two lines of distance Δ in a rectangle area of length $l = 10{,}000$ meters, according to the LNRO distribution. The sensors are equally divided into the two deployment lines. The width of the field is chosen to be large enough so that all the nodes fall into the rectangle in the simulations. We consider four different offset variance values: $\sigma = 5$, 10, 15, and 30. Each data entry in Figure 10 is an average over 1000 experiments.

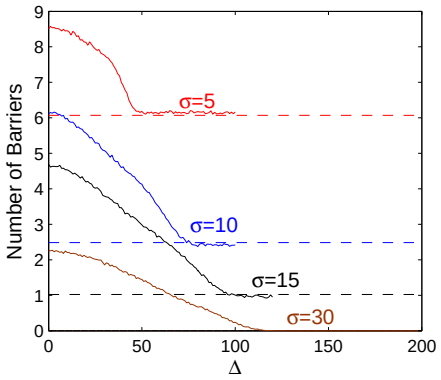

Fig. 10. Barrier coverage of a two-line deployed sensor network.

Figure 10 plots the number of barriers as a function of Δ for the four offset variance values. The $\Delta = 0$ cases correspond to the scenario where the two deployment lines coincides with each other. Thus the effect is equivalent to the case when the same number of sensors are deployed along a single line. We observe that the number of disjoint barriers decreases as the distance Δ increases. This can be explained as follows. When the two lines are close to each other, there is a significant overlap between the two groups of sensors,

as shown in Figure 9(a). A sensor in one group can connect to sensors in its own group as well as sensors in its neighboring group, increasing the chances of barrier formation. As Δ increases, i.e., as the two deployment lines become farther apart from each other, there is less overlap between the two groups of sensors, resulting in a degraded barrier coverage.

In particular, when Δ increases to roughly $(6\sigma + 2r)$, the number of barriers levels off to about twice that of a single line deployment with half of the sensors (dashed lines). At this distance, there is almost no overlap between the two groups of sensors, and the probability of forming barriers using sensors from both groups diminishes.

VII. Conclusion

We study the barrier coverage of a wireless sensor network where sensors are deployed along lines with normally distributed random offsets. We establish a tight lower bound for the existence of barrier coverage under LNRO. We find that sensor deployment strategies have direct impact on the barrier coverage of a wireless sensor network. Different deployment strategies may yield significantly different barrier coverage. In particular, when the variance of the random offset in LNRO is relatively small compared to the sensor's sensing range, the barrier coverage of LNRO significantly outperforms that of the Poisson model. We also study the multiple-line deployment scenario and investigate how barrier coverage depends on the distance between adjacent lines and the random offsets of sensors.

Our results suggest that in the planning and deployment of wireless sensor networks, the coverage goal and possible sensor deployment strategies must be carefully examined. The results obtained in this paper provide important guidelines to the deployment and performance of wireless sensor networks for barrier coverage.

VIII. Acknowledgment

We thank the anonymous reviewers for their helpful comments. We would also like to thank Dr. Haralabos Papadopoulos for pointing out useful references. Benyuan Liu was partly supported by the National Science Foundation under grant CNS-0721626. Jie Wang was supported in part by NSF under grants CNS-0709001 and CCF-0830314.

References

[1] D. Gage, "Command control for many-robot systems," in *Proc. of the Nineteenth Annual AUVS Technical Symposium (AUVS-92)*, 1992.

[2] S. Kumar, T. H. Lai, and A. Arora, "Barrier coverage with wireless sensors," in *Proc. ACM Mobicom*, 2005.

[3] U. Berkeley and M. Co, "Tracking vehicles with a uav-delivered sensor network," http://www-bsac.eecs.berkeley.edu/∼pister/29Palms0103/.

[4] A. Saipulla, B. Liu, and J. Wang, "Barrier coverage with airdropped sensors," in *Proc. of IEEE MilCom*, 2008.

[5] A. Chen, S. Kumar, and T.-H. Lai, "Designing localized algorithms for barrier coverage," in *Proceedings of ACM Mobicom*, 2007.

[6] B. Liu, O. Dousse, J. Wang, and A. Saipulla, "Strong barrier coverage of wireless sensor networks," in *Proc. of The ACM International Symposium on Mobile Ad Hoc Networking and Computing (MobiHoc)*, 2008.

[7] S. Meguerdichian, F. Koushanfar, M. Potkonjak, and M. B. Srivastava, "Coverage problems in wireless ad-hoc sensor networks," in *Proc. IEEE Infocom*, 2001, pp. 1380–1387.

[8] X.-Y. Li, P.-J. Wan, and O. Frieder, "Coverage in wireless ad-hoc sensor networks," *IEEE Transactions on Computers*, vol. 52, no. 6, pp. 753–763, June 2003.

[9] G. Veltri, Q. Huang, G. Qu, and M. Potkonjak, "Minimal and maximal exposure path algorithms for wireless embedded sensor networks," in *Proc. of ACM Sensys*, 2003.

[10] T. Clouqueur, V. Phipatanasuphorn, P. Ramanathan, and K. K. Saluja, "Sensor depolyment strategy for detection of targets traversing a region," *ACM Mobile Networks and Applications*, vol. 8, p. 453C461, 2003.

[11] E. Amaldi, A. Capone, M. Cesana, and I. Filippini, "Coverage planning of wireless sensors for mobile target detection," in *Proc. of IEEE MASS*, 2008.

[12] B. Liu and D. Towsley, "A study on the coverage of large-scale sensor networks," in *The 1st IEEE International Conference on Mobile Ad-hoc and Sensor Systems*, 2004.

[13] P. Balister, B. Bollobas, A. Sarkar, and S. Kumar, "Reliable density estimates for coverage and connectivity in thin strips of finite length," in *Proceedings of ACM Mobicom*, 2007.

[14] A. Chen, T. H. Lai, and D. Xuan, "Measuring and guaranteeing quality of barrier-coverage in wireless sensor networks," in *Proc. of The ACM International Symposium on Mobile Ad Hoc Networking and Computing (MobiHoc)*, 2008.

[15] "Crossbow Technology INC." http://www.xbow.com/.

[16] E. Gilbert, "Random plane networks," *J. SIAM*, vol. 9, pp. 533–543, 1961.

[17] J. Proakis, *Digital Communications: Fourth Edition*. McGraw-Hill, 2000.

[18] T. H. Cormen, C. E. Leiserson, R. L. Rivest, and C. Stein, *Introduction to Algorithms (Second Edition)*. MIT Press and McGraw-Hill, 2001.

Appendix

A. Proof of Theorem 4.1

Consider now the relative positions of nodes s_i and s_{i+1}. Define $z^x = s^x_{i+1} - s^x_i$ and $z^y = s^y_{i+1} - s^y_i$. Then $z^x = \zeta + \delta^x_{i+1} - \delta^x_i$ and $z^y = \delta^y_{i+1} - \delta^y_i$. Since the δ^s are Normally distributed with variance σ^2, then $\delta^x_{i+1} - \delta^x_i$ and $\delta^y_{i+1} - \delta^y_i$ are both Normal random variable with variance $2\sigma^2$, i.e., $z^x \sim N(\zeta, 2\sigma^2)$ and $z^y \sim N(0, 2\sigma^2)$.

The distance between s_i and s_{i+1} is equal to:

$$d_i \triangleq |s_{i+1} - s_i| = \sqrt{(z^x)^2 + (z^y)^2} \tag{8}$$

This implies that d_i follows a Ricean distribution. Since the distribution is identical for all i, we drop the index and denote the distance between two consecutive nodes as d.

In particular, the probability that $d < \rho$ is given by (see for instance [17], Chapter 2):

$$P(d < \rho) = 1 - Q_1(\frac{\zeta}{\sqrt{2}\sigma}, \frac{\rho}{\sqrt{2}\sigma}) \quad (9)$$

where Q_1 is the Marcum's Q-function of the first order, defined by:

$$Q_1(\frac{\zeta}{\sqrt{2}\sigma}, \frac{\rho}{\sqrt{2}\sigma}) = e^{-(\zeta^2+\rho^2)/4\sigma^2} \sum_{k=0}^{\infty} \left(\frac{\zeta}{\rho}\right)^k I_k\left(\frac{\zeta\rho}{2\sigma^2}\right) \quad (10)$$

and I_k is the k-th order modified Bessel function of the first kind.

Thus, two sensors s_i and s_{i+1} provide barrier coverage with probability $P(d < \rho)$. If each pair of sensors s_i and s_{i+1} is within ρ of each other and within ρ of the boundary, then the sensor deployment provides barrier coverage over the all width of the area. For all $1 \leq i \leq n-1$, denote by W_i the event that $d_i < \rho$. Denote by W_0^b the event that s_1 is within distance ρ of the boundary $x = 0$, and W_n^b that s_n is within distance ρ of the boundary $x = l$. Since this is not the only configuration that provides barrier coverage, we have

$$P(\text{Barrier Coverage}) \geq P\left(W_0^b \bigcap W_n^b \bigcap (\bigcap_{i=1}^{n-1} W_i)\right). \quad (11)$$

Assumption 1) allows us to consider W_0^b, W_n^b and W_i, $1 \leq i \leq n-1$, as independent events and approximate $P(W_0^b \bigcap W_n^b \bigcap (\bigcap_{i=1}^{n-1} W_i))$ with $P(W_0^b)P(W_n^b)(P(d < \rho))^{(n-1)}$. Indeed, if assumption 1) was violated, and ρ was almost equal to ζ, then a perturbation which brings node s_i close to s_{i-1} would also create a gap between s_i and s_{i+1}. W_i happening thus implies that W_{i+1} would not happen, and that both events are conditioned on each other, not independent. However, by choosing the right parameter κ, the approximation by independent events is appropriate, as we confirm in the evaluation section.

We can also easily verify that $P(W_0^b) > P(d < \rho)$ and symmetrically, $P(W_n^b) > P(d < \rho)$, so that $P(\text{Barrier Coverage}) \geq P(d < \rho)^{n+1}$.

Assumption 2) ensures that the gap between $P(BarrierCoverage)$ and $P(\bigcap_{i=0}^{n} W_i)$ stays limited, and that the most likely configuration to provide coverage is indeed by having each s_i and s_{i+1} within ρ of each other. Other configurations are possible, and a gap between s_i and s_{i+1} could be filled by having a third sensor out of position in the sequential ordering along the x-axis. However, assumption 2) ensures that such other configurations have a low likelihood. Simulation will show that, under assumption 2) the lower bound is actually tight.

Note that we do not put an explicit dependency of ζ on n, but as $n \to \infty$, the probability of barrier coverage goes to 1 as $\zeta \to 0$, all other parameters being constant.

B. Barrier Construction Algorithm

We now present the algorithm to compute the number of barriers in a sensor network. We assume that the location of each sensor is collected prior to computation. We first construct a graph based on the senor location information, then compute the maximum flow of the graph.

Algorithm to Construct Barriers:

1) Construct a flow graph $G(V,E)$ as follows. Each vertex in V represents a sensor node. For any two vertices u and v in V, if their sensing areas overlap, add edge (u,v) in E.
2) From $G(V,E)$, construct a weighted directional graph $G^*(V^*,E^*)$ as follows. For any node n_i in V, add n_i' and n_i'' to V^*, and an edge (n_i', n_i'') to E^*. If edge (n_i, n_j) exists in E, add edges (n_i'', n_j') and (n_j'', n_i') to E^*. Add two new vertices s and d into V^*. For any node n_i in V, if its sensing range intersects the left boundary of the area, add edge (s, n_i') to E^*; if its sensing range intersects the right boundary of the area, add edge (n_i'', d). The capacity of each edge in E^* is set to 1. For each edge in E^*, add its reverse edge to E^*, and set the capacity of this new edge to 0.
3) Compute the maximum flow from s to d in graph $G^*(V^*,E^*)$ using a standard algorithm (e.g., Ford-Fulkerson, Edmond-Karp, or the relabel-to-front algorithms [18]).

Note that in Step 2, each sensor is mapped to two graph nodes with one edge between them. This is to guarantee that each sensor node is only used once in barrier construction. In Step 3, each augmenting path forms a barrier in the sensor network. The maximum flow of grapth G^* will give the number of disjoint barriers in the original sensor network.